NeuroImage 270 (2023) 119959

Contents lists available at ScienceDirect

NeuroImage

journal homepage: www.elsevier.com/locate/neuroimage

Towards an optimization of functional localizers in non-human primate neuroimaging with (fMRI) frequency-tagging

Marie-Alphée Laurent[a,1,*], Pauline Audurier[b,1], Vanessa De Castro[b], Xiaoqing Gao[c], Jean-Baptiste Durand[b], Jacques Jonas[a,d], Bruno Rossion[a,2], Benoit R. Cottereau[b,2,*]

[a] Université de Lorraine, CNRS, CRAN, F-54000 Nancy, France
[b] Centre de Recherche Cerveau et Cognition, Université Toulouse 3 Paul Sabatier, CNRS, 31052 Toulouse, France
[c] Center for Psychological Sciences, Zhejiang University, Hangzhou City, China
[d] Universite de Lorraine, CHRU-Nancy, Service de neurologie, F-54000, France

ARTICLE INFO

Keywords:
Face recognition
Macaque
FMRI
Vision
Non-human primate
Frequency-tagging

ABSTRACT

Non-human primate (NHP) neuroimaging can provide essential insights into the neural basis of human cognitive functions. While functional magnetic resonance imaging (fMRI) localizers can play an essential role in reaching this objective (Russ et al., 2021), they often differ substantially across species in terms of paradigms, measured signals, and data analysis, biasing the comparisons. Here we introduce a functional frequency-tagging face localizer for NHP imaging, successfully developed in humans and outperforming standard face localizers (Gao et al., 2018). FMRI recordings were performed in two awake macaques. Within a rapid 6 Hz stream of natural non-face objects images, human or monkey face stimuli were presented in bursts every 9 s. We also included control conditions with phase-scrambled versions of all images. As in humans, face-selective activity was objectively identified and quantified at the peak of the face-stimulation frequency (0.111 Hz) and its second harmonic (0.222 Hz) in the Fourier domain. Focal activations with a high signal-to-noise ratio were observed in regions previously described as face-selective, mainly in the STS (clusters PL, ML, MF; also, AL, AF), both for human and monkey faces. Robust face-selective activations were also found in the prefrontal cortex of one monkey (PVL and PO clusters). Face-selective neural activity was highly reliable and excluded all contributions from low-level visual cues contained in the amplitude spectrum of the stimuli. These observations indicate that fMRI frequency-tagging provides a highly valuable approach to objectively compare human and monkey visual recognition systems within the same framework.

1. Introduction

For decades, the macaque monkey has been used to better understand visual processing in humans as this animal model permits invasive explorations of neural activity (e.g., from single or multi-unit recordings), and the functional organization of the two species' visual system is thought to be largely similar (Jacobsen et al., 1936; Passingham, 2009; Krug and Parker, 2017). At the highest levels of visual processing, early electrophysiological studies revealed neurons responding selectively to faces in the macaque inferotemporal cortex (IT; Gross et al., 1972; Perrett et al., 1982; for reviews of these early studies, see Desimone et al., 1991), and it is generally believed that the characterization of these neurons' operations can clarify the neural basis of human face recognition (Barraclough and Perrett, 2011).

With the emergence of functional magnetic resonance imaging (fMRI), which can now be performed in both humans and macaques, it is henceforth possible to establish cross-species correspondence and identify homologous functional brain regions in the two species (Orban et al., 2004; Vanduffel and Farivar, 2014). As a consequence, following the identification of face-selective regions in the human occipito-temporal cortex with functional magnetic resonance imaging (fMRI) (Puce et al., 1995; see Sergent et al., 1992 for earlier neuroimaging studies with positron emission tomography), functional localizers were developed to identify and characterize face-selective regions in both humans (Kanwisher et al., 1997; Haxby et al., 2000) and macaques (Tsao et al., 2003; Pinsk et al., 2005; and also in marmosets Hung et al., 2015). Subsequently, macaque face-selective regions have been explored using electrophysiological recordings or microstimulation to gain insight

* Corresponding authors.
E-mail addresses: marie-alphee.laurent@univ-lorraine.fr (M.-A. Laurent), benoit.cottereau@cnrs.fr (B.R. Cottereau).
[1] These authors contributed equally to this work.
[2] Co-senior authors.

https://doi.org/10.1016/j.neuroimage.2023.119959.
Received 9 September 2022; Received in revised form 16 February 2023; Accepted 20 February 2023
Available online 22 February 2023.

the cellular basis of primate face recognition (e.g., Tsao et al., 2006; Moeller et al., 2008; Freiwald et al., 2009; Freiwald and Tsao, 2010; Issa and DiCarlo, 2012; Taubert et al., 2015; Aparicio et al., 2016; Chang and Tsao, 2017; Moeller et al., 2017; Taubert et al., 2018). This specific line of research on the neural basis of primate face recognition illustrates the importance of common functional localizers in fMRI to enhance cross-species neuroscience imaging research (Russ et al., 2021).

However, three decades of research have brought considerable variability between functional fMRI localizers employed in different studies, within and across species, which greatly complicates the correspondence between the obtained results. For instance, in humans, face localizers differ in terms of many factors such as the contrasting stimuli, event and block durations, task conditions (e.g., passive viewing or n-back memory task), the brain volume measured, statistical criteria, etc. (e.g., Kanwisher et al., 1997; Haxby et al., 1999; Ishai et al., 2005, 2008; Fox et al., 2009; Rossion et al., 2012; Weiner and Grill-Spector, 2013; Zhen et al., 2015). Although systematic comparisons of the effects of these variable factors are lacking, these differences undoubtedly contribute to variations in the extent, localization, strength, and reliability of face-selective activations observed in the human occipito-temporal cortex across studies (Duncan et al., 2009; Berman et al., 2010; Rossion et al., 2012).

Interestingly, despite the much smaller number of research groups performing fMRI recordings in macaques, face localizers also differ substantially across monkey studies regarding paradigm designs, measured signals, and data analysis. Most of the time, experimental paradigms are based on block-design contrasting face and non-face objects, although event-related designs are used as well (Tsao et al., 2003; Pinsk et al., 2005, 2008a,2008b; Hadj-Bouziane et al., 2008; Pinsk et al., 2009; Bell et al., 2011; Russ and Leopold, 2015; Premereur et al., 2016; Livingstone et al., 2017; Taubert et al., 2020, 2022). In addition, the number of runs performed for each animal and the duration of these runs can also vary substantially from one study to another. Altogether, these differences may contribute to variability in the number, size, and anatomical localization of face-selective clusters across studies. As a matter of fact, while three then six face-selective regions were initially reported in the posterior, middle, and anterior parts of the superior temporal sulcus (STS), either in its fundus or on its lower bank (Tsao et al., 2003, 2008a), more recent studies revealed additional activations. These have notably been observed in the upper bank of the STS, the perirhinal cortex, the entorhinal cortex, the parahippocampal cortex, the amygdala, and the hippocampus, with up to ten face-selective regions in the temporal lobe, varying across individual animals (Ku et al., 2011; Fisher and Freiwald, 2015; Landi and Freiwald, 2017; Hesse and Tsao, 2020).

In addition to these intra-species variabilities, there are important inter-species differences between the typical face localizer paradigms used in humans and macaques in terms of stimuli, tasks, durations, and statistical criteria. For instance, while human faces are systematically used in human fMRI studies, either human (Freiwald and Tsao, 2010) or monkey faces (Hadj-Bouziane et al., 2008; Bell et al., 2009; Ku et al., 2011; Janssens et al., 2014; Fisher and Freiwald, 2015; Hung et al., 2015; Arcaro et al., 2017; Livingstone et al., 2017) or both (Tsao et al., 2003, 2008a,2008b; Pinsk et al., 2009; Issa and DiCarlo, 2012; Premereur et al., 2016; Taubert et al., 2020) are used in monkey fMRI studies. Furthermore, although it has been claimed that using human or monkey faces in face localizers performed in monkeys has little influence on brain activations (Russ et al., 2021), with the exception of a few studies (Murphy and Leopold, 2019), no systematic comparison has been performed to our knowledge. Another key factor that limits cross-species comparisons is that monkey fMRI recordings are almost systematically performed using a contrast agent (MION or USPIO particles see e.g., (Rajimehr et al., 2009; Tsao et al., 2008a; Janssens et al., 2014; Arcaro et al., 2020; Taubert et al., 2020) while human experiments rely on blood-oxygen-level dependent (BOLD) imaging, with a different impulse response function (IRF; Leite et al., 2002).

To circumvent these issues and contribute to developing common fMRI functional localizers that will enhance cross-species neuroscience imaging research (Russ et al., 2021), here we introduce a recently validated functional face localizer in humans (Gao et al., 2018) for NHP neuroimaging. As in the very first human fMRI studies on face perception (Puce et al., 1995, 1996), this face localizer is based on the principle of frequency-tagging, with face-selective activity identified objectively in the frequency spectrum at a periodic rate of face stimulation among non-face objects (Gao et al., 2018, 2019). Compared to other face localizers, this paradigm does not require IFR modeling, and relies on widely variable natural images (providing high ecological validity), for both faces and non-face objects in order to naturally control for low-level cues' contribution to categorical differences (Rossion et al., 2015). Furthermore, in humans, this paradigm shows a very high sensitivity and test-retest reliability (Gao et al., 2018, see also Gao et al., 2019, 2022).

Here we characterized the set of face-selective regions, i.e., the cortical face network, of two macaques using exactly the same paradigm as previously used in humans, with natural photographs of objects and faces. We also compared human to monkey faces and evaluated the putative contribution of low-level visual cues through a phase-scrambled control. Moreover, the fast rate of stimulation ensured that only one gaze fixation was performed on each stimulus, eliminating the contribution of potential eye gaze exploration differences between species. From an analysis in the Fourier domain, we identified face-selective clusters with a high signal-to-noise ratio (SNR) in both monkeys, at typical locations, and we demonstrated that our results are robust and reproducible. To promote this new approach as a standard localizer of face-selective regions in NHP, the experimental paradigm, stimuli, and analysis scripts will be provided online (Open Science Framework) upon acceptance of the paper.

2. Materials and methods

2.1. Subjects

Two female rhesus macaques M01 and M02 (age: 11–20 years; weight: 5.30–6.15 kg) were involved in this study. This project received authorization from the French Ministry of Research (MP/03/04/10/09) and was approved by a local ethics committee (CNREEA code: C2EA - 14). Animal housing, handling, and all the experimental protocols such as surgery, behavioral training, and fMRI recordings were conducted with respect to the European Union legislation (2010/63/UE) and to the French Ministry of Agriculture guidelines (décret 2013–118). As required and recommended for primate welfare, each of the two animals was housed in a social group of individuals in a spacious and enriched enclosure and could thus develop species-specific behavior such as foraging and congeners delousing.

2.2. Visual stimulation

The stimuli used in the present study consisted of color images of human faces, monkey faces, and non-face objects from a wide variety of categories (e.g., houses, cars, animals, etc.; Fig. 1). The set included natural images (i.e., unsegmented) of 100 different and non-famous human faces and 195 non-face objects images from the dataset created by Rossion and colleagues at the *Face Categorization Lab* of the University of Louvain, Belgium (from Gao et al., 2018). The monkey face images were 89 natural photographs of rhesus macaques collected on the internet, thus unfamiliar to the macaque subjects. Each face image contained only a single human or monkey face. Face and object images significantly varied in size, lighting conditions, color, 3D orientation, and background (Fig. 1). Unlike when using highly homogenous sets of stimuli, this variability minimizes the contribution of low-level cues to face-selective neural responses and ensures that these responses reflect generalization across variable exemplars (i.e., a category-selective response; Rossion et al., 2018).

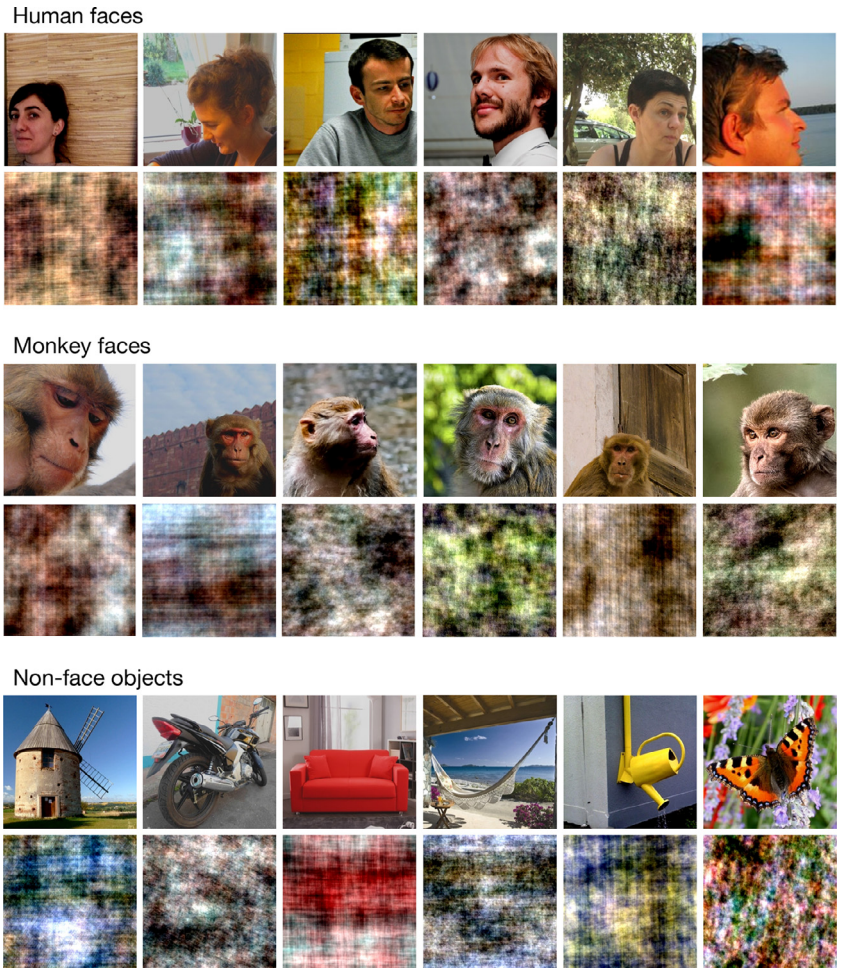

Fig. 1. Example stimuli. Our dataset contained natural photographs of human (upper rows) and monkey (middle rows) faces and of non-face objects (lower rows). These stimuli differed in size, lighting condition, color, 3D orientation, and background. Phase-scrambled versions of the images in the Fourier domain (below each face and object image) were also included as control conditions.

To further control for the potential contribution of low-level visual cues to category-selective responses, the stimuli were resized to 256 × 256 pixels and equalized in terms of intensity and contrast (averages values of 115 ± 0.7 and 0.56 ± 0.02 were used). Note that this last procedure did not homogenize low-level differences between faces and objects inside the global images (see Supplementary Fig. 1 for a characterization of the low-level properties in these image sets). To ensure full control of low-level properties, a phase-scrambled version of each image was also created by randomizing the phase of the original images in the Fourier domain, as in previous human EEG (Rossion et al., 2015; Gao et al., 2018) and monkey fMRI (Audurier et al., 2022) studies. These scrambled images had the same low-level visual information (amplitude spectrum; e.g., Honey et al., 2008) as the originals, but without any recognizable structure (Fig. 1).

2.3. MRI recordings

Recordings were performed on a 3 Tesla MR scanner (Philips Achieva) using a dedicated custom 8-channel phased array coil (RapidBiomed) specially designed to fit the skull of our animals while preserving their field of view.

2.3.1. Recordings for individual templates of reference

Four T1-weighted anatomical volumes were acquired during a single session prior to the study for each monkey at a high resolution (MPRAGE; repetition time, TR = 10.3 ms; echo time, TE = 4.6 ms, flip angle = 8°; FOV: 155 × 155 mm; matrix size: 312 × 192 mm; voxel size = 0.5 × 0.5 × 0.5 mm; 192 sagittal slices acquired in an interleaved order), as well as 300 functional volumes (gradient-echo EPI; TR = 1500 ms, TE = 30 ms, flip angle = 75°, SENSE factor = 1.6; FOV: 100 × 100 mm; matrix size: 68 × 64 mm; voxel size = 1.25 × 1.25 × 1.5 mm, 32 axial slices with a thickness of 1.5 mm and no gap). For our two macaques, those volumes were acquired under slight anesthesia (Zoletil 100:10 mg/kg and Domitor: 0.04 mg/kg) during which the animal constants were monitored with an MR-compatible oximeter. Anatomical and functional individual reference templates were then built from those acquisitions (see Cottereau et al., 2017 for more details).

2.3.2. Functional recordings

The functional recording sessions were performed on awake, behaving macaques on a daily basis and lasted about 1 h (10–14 runs). The animals were head-fixed, seated in a sphinx position within an MRI-compatible primate chair facing a screen at a viewing distance of 55 cm. Visual stimuli were projected on this screen at a spatial resolution of 1024 × 768 pixels and a frame rate of 60 Hz. They consisted of square images (see above) of 14,6 × 14,6° of visual angle. The animals were involved in a passive fixation task while the position of one eye was monitored using an infrared video-based eye-tracking setup (Cambridge Research). They were rewarded with water when their gaze was maintained within a central fixation window of 2 × 2°. During a run, images of non-face objects were displayed in random order (without immediate repetition of the same image) on the screen at a rate of 6 Hz (i.e., 6 images/*sec*), for 243 s (162 TRs). Every 9 s (i.e., at $F = 0.111$ Hz), seven randomly selected images from the target category (human faces or monkey faces) were presented. Importantly, these face images alternated with six images of non-face objects for 2.167 s (Fig. 2) to avoid category (i.e.,

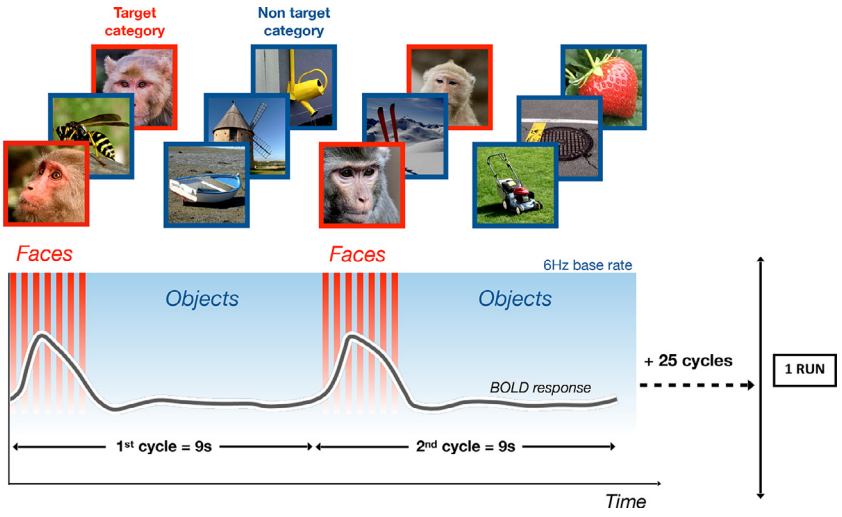

Fig. 2. Illustration of the Fast Periodic Visual Stimulation localizer. The protocol is based on a rapid periodic presentation of visual stimuli at 6 Hz. At the beginning of each cycle of 9 s, a "burst" of stimuli from the target category (illustrated in red) is presented for 2.167 s. This burst contains seven faces (e.g., monkey faces on the figure) alternating with six non-face objects from the non-target category (illustrated in blue). Stimuli from the non-target category are presented for the rest of the cycle. A run is composed of 27 cycles and lasts 243 s. In gray, the expected BOLD response for a voxel selective to the target category. This periodic category-selective response can be objectively detected in the Fourier domain.

face) adaptation and maximize the contrast between faces and objects (i.e., the face-selective response). Since bursts of faces were displayed at a fixed frequency of 0.111 Hz, systematic deviations from the baseline activity to non-face objects, i.e., face-selective responses, could be directly extracted in the Fourier domain at this frequency (Regan, 1966; see Gao et al., 2018; see also Puce et al., 1995 for an application of this approach in the first fMRI face localizer study).

To assess the potential contribution of low-level visual cues in the results (see the "*Visual stimulation*" section above), we also included control runs with phase-scrambled versions of faces and non-faces images. These runs were acquired separately. The whole experiment (i.e., visual display, eye monitoring, and water reward) was monitored using the EventIDE software (Okazolab).

Functional images were collected with a T2* weighted gradient-echo echoplanar imaging (EPI) sequence (TR = 1500 ms, TE = 30 ms, flip angle = 75°, SENSE factor = 1.6; multi-band (MB) = 2; FOV: 100 × 100 mm; matrix size: 68 × 64 mm; voxel size = 1.25 × 1.25 × 1.5 mm).

2.4. Data processing

2.4.1. Anatomical and functional templates

Data collected during the anesthetized sessions were used to create individual functional and anatomical templates. The anatomical template was obtained by realigning and averaging the four T1-weighted (MPRAGE) volumes. It was then aligned to the MNI space of the 112RM-SL (McLaren et al., 2009, 2010). Cortical surface reconstructions were performed using the CARET software (Van Essen et al., 2001). The functional template was obtained by realigning and averaging the 300 functional (GE-EPI) volumes. It was then aligned with the anatomical template. Spatial normalization parameters (affine and non-rigid) between the functional and anatomical templates were determined based on the gray matter probability maps of both templates.

2.4.2. Preprocessing of the functional data

In order to minimize the influence of eye movements on BOLD signal fluctuations, only runs with fixation rates above 85% were considered for further analyses. For our two monkeys (M01 and M02), we collected 20 runs for each condition of the face localizer (i.e., 20 runs with human faces and 20 with monkey faces). We also collected 14 control runs with phase-scrambled versions of faces (7 runs with phase-scrambled versions of human faces and 7 other runs with phase-scrambled versions of monkey faces) and non-faces objects. Fewer runs were recorded in this case since, as shown below in the "Results" section, it was largely enough to demonstrate that our face-selective responses were not driven by low-level visual cues. The volumes of each run were first rigidly realigned with each other, and a mean functional image of the runs was computed for co-registration with the functional template. All the individual images of the runs were then resliced to be brought into the space of the animal's anatomical space by combining (1) the individual rigid realignment parameters, (2) the affine co-registration parameters between the mean run image and the functional template, (3) the predefined spatial normalization parameters (affine and non-rigid) between the functional and anatomical templates. Individual images were also up-sampled at 1 mm isotropic voxels during the interpolation step. Since we used multi-band fMRI sequences, no slice timing correction was applied. To reduce noise in the recordings, a principal component analysis (PCA) was performed on the time courses of voxels located outside the brain (see Vanduffel and Farivar 2014 or Héjja-Brichard et al., 2020). Time courses in those voxels mostly reflect artifacts caused by the movement of the animals and are independent of our experimental design. For each run, the 20 first principal vectors were regressed out of the data. All the preprocessing of the data was performed using MATLAB software (MathWorks®).

2.4.3. Fourier analysis and amplitude of face-selective responses

For each condition, pre-processed fMRI data were first averaged across runs in the volumetric space. The corresponding 243 s time courses contained 27 cycles of our 9 s stimulus (see above). We removed the first cycle (9 s) to discard start-up transients (see e.g., Cottereau et al., 2012), leading to average time-courses of 234 s (i.e., 26 cycles of our stimulus) which were projected onto the individual cortical surfaces using a trilinear interpolation along the surface nodes (5 sampling points per node along their normal vector; from −0.5 mm to +0.5 mm). The 5 functional time courses were averaged together in a single mean time course attributed to the surface's node. Data were subsequently smoothed in the cortical surface space using an iterative (n = 8) dilation process. The value at each node was estimated from the average of the responses in its first-order neighborhood. Next, average time courses in the cortical surface space were analyzed following the procedure described in Gao et al. (2018). We performed a Fourier analysis using the FFT function in Matlab without windowing. This Fourier analysis was performed on the entire 234 s time-courses and therefore had a frequency resolution of 1/234 = 0.0043 Hz. Because our stimulus period (9 s) was a multiple of our sampling rate (TR = 1.5 s) and our analysis window contained a large (>10) and integer number of stimulus periods (234 s = 26 cycles of 9 s), this approach avoids overspill artifacts and minimizes the influence of trend artifacts (Bach and Meigen, 1999). The amplitude spectrum was directly derived from the Fourier transform coefficients. We subsequently converted the amplitudes at the face stimulation frequency (i.e., F = 0.111 Hz) and its second harmonic (2F = 0.222 Hz) into Z-scores as in previous studies

(McCarthy et al., 1994; Puce et al., 1995), using the mean and standard deviation of the amplitude at neighboring frequencies:

$$Z - score = (A_S - \mu_N)/\sigma_N$$

where A_S is the amplitude at the face frequency stimulation (or at the second harmonic), μ_N and σ_N are the mean and standard deviation across the corresponding 20 neighboring frequency bins (10 on each side, with a bin width of 0.0043 Hz; e.g., Rossion et al., 2015; Jonas et al., 2016). The overall Z-score was calculated by summing the baseline-subtracted amplitudes at the stimulation frequency and the second harmonic (Retter et al., 2021). This procedure was applied to the time course of each cortical node independently.

2.4.4. Characterization of face-selective clusters

In each of our two macaques, we identified face-selective clusters on the Z-scores maps estimated from the 40 runs of our (human and monkey) face localizer. We only considered clusters with significant activations in both hemispheres. The MNI coordinates (see Table 1) of these clusters were given by those of their local maxima. Their Z-scores (respectively amplitude spectra, see Fig. 3) were obtained by averaging together the Z-scores (respectively amplitude spectra) of the local maxima and their third-order neighborhoods on the cortical tessellation (covered on average by 15 nodes).

To avoid double-dipping effects (Kriegeskorte et al., 2009) in our statistical comparison between responses to face stimuli and their phase-scrambled versions, we defined a new set of face-selective clusters from the Z-scores obtained in the odd runs. We then compared the Z-scores obtained in these face-selective clusters during the even runs to those obtained during the phase-scrambled controls. Responses to face stimuli were considered as significantly higher for differences of Z-scores greater than 3.

To avoid double-dipping in the statistical comparison between responses to human versus monkey faces (see Fig. 7), we estimated the Z-scores of responses to monkey faces within face patches defined from runs with human faces and Z-scores of responses to human faces within face patches defined from runs with monkey faces (see Supplementary Table 1). Data used to define the face patches and estimate the Z-scores are therefore independent.

2.4.5. Test-retest reliability

To assess the reliability of the paradigm, we performed the analyses on two subsets, defined from the even and odd runs of our data. We quantified the overlap between the face-selective nodes identified in the two datasets using the Dice coefficient (as in Gao et al., 2018), a measure of the extent of overlap between the two thresholded activation maps obtained:

$$O_{ij} = 2 \times V_{ij}/(V_i + V_j)$$

where O_{ij} is the consistency score between even run i and odd run j, V_{ij} is the number of face-selective nodes in both datasets, V_i is the number of face-selective nodes in even run i, and V_j is the number of face-selective nodes in odd run j. We calculated three scores of consistency within each animal's anatomically defined STS: on the unthresholded data, on the thresholded activation maps at $Z = 3$, and on the activation maps presented in our figures (see the "Results" section, $Z = 7$ for M01 and $Z = 4$ for M02). We also calculated these consistency scores at the whole-brain level, within the activations defined from 14 runs, and the analysis performed on the 12 even and 12 odd remaining runs. In addition, correlation analyses were used to assess the degree of the correspondence between the activations obtained from these subsets of the data.

3. Results

This study aimed to demonstrate the efficacy of a frequency-tagging technique recently developed for human neuroimaging protocols (Gao et al., 2018) in a non-human primate (NHP) model. We applied the Fast Periodic Visual Stimulation localizer (see Fig. 2) to identify the cortical face network in two awake behaving macaques (M01 and M02). Stimuli were constructed using natural photographs of objects and either human or monkey faces (see Fig. 1). fMRI data were analyzed in the frequency domain (see the "Materials and methods" section).

Table 1
MNI coordinates (in mm) of the local maxima for the face-selective clusters identified in both hemispheres of the two animals.

ROI		M01			M02		
		x	y	z	x	y	z
ML	L	−18.9	6.3	9.1	−23.8	5.3	9.2
	R	20.1	3.1	12.6	24.2	6.8	8.8
MF	L	−20.9	7.6	10.2	−20.6	5.1	6.8
	R	24.5	6.1	13.9	22.8	5.9	6.6
PL	L	−24.8	3.4	17.5	−25.9	2.1	12.6
	R	17.3	1.2	16.7	21.3	1.7	12.2
AL	L	−23.1	13.8	3.3			
	R	24.2	12.7	4.3			
AF	L	−18.7	16.3	5.3			
	R	19.5	15.3	6.2			
PO	L	−14.2	38.6	20.4			
	R	13.7	40.1	21.1			
PVL	L	−16.2	26.2	19.5			
	R	16.9	28.1	19.6			

3.1. Face-selective clusters in macaque monkeys

Fig. 3-A presents face-selective activations projected on inflated reconstructions of the left and right cortical hemispheres of M01 and M02. These activations were estimated from all the runs with human and monkey faces combined (differences between activations in response to human versus monkey faces are discussed in Section 3.3.). Red-to-yellow colors indicate significantly different BOLD responses to face than to non-face objects, under the form of Z-scores (see the "Materials and Methods" section). Only lateral views are shown as we did not observe significant activations on medial and ventral cortices (see Supplementary Fig. 2). Clusters with strong face-selective responses were observed along the superior temporal sulcus (STS) of the two hemispheres in both monkeys (Z-score > 7 for M01, $p < 10^{-10}$ uncorrected, and Z-score > 4 for M02, $p < 10^{-5}$ uncorrected). These clusters were mainly localized in the middle fundus (MF) of the STS and in the middle lateral (ML) and posterior lateral (PL) parts of its lower banks, in agreement with face-selective regions described in previous monkey fMRI studies (e.g., Aparicio et al., 2016; Livingstone et al., 2017), although in M01, the PL cluster was a little bit deeper in the fundus of the STS. In M01, we also found two additional clusters in the anterior fundus (AF) and the anterior lateral (AL) parts of the STS (as in Lafer-Sousa and Conway, 2013; Taubert et al., 2020). Face-selective activations were also observed in the anterior medial (AM) part of this monkey's STS (as in Ku et al., 2011; Issa and DiCarlo, 2012; Arcaro et al., 2017) but only in the right hemisphere. Significant activations were found in the prefrontal orbital (PO) and the prefrontal ventrolateral (PVL) cortices of M01 (see Fig. 4-A), in agreement with (Tsao et al., 2008b; Janssens et al., 2014). Activations in the PVL cluster were also found in M02 (Z-score > 6 at the local maxima), although their spatial extent remained limited. Coronal slices presenting Z-scores in the face-selective clusters of the STS and prefrontal cortex are respectively shown in Figs. 3-B and 4-B. MNI coordinates of the local maxima in these clusters are provided in Table 1.

Face-selective regions in M01 and M02 were generally in good agreement with those reported in previous monkey fMRI studies (Janssens et al., 2014; Hesse and Tsao, 2020 for review). In both animals, ML and MF were the clusters with the highest face-selective responses (Z-score > 25 for M01, Z-score > 12 for M02; in line with Pinsk et al., 2009 and Freiwald and Tsao, 2010). However, there was also an important variability in the number and extent of face-selective

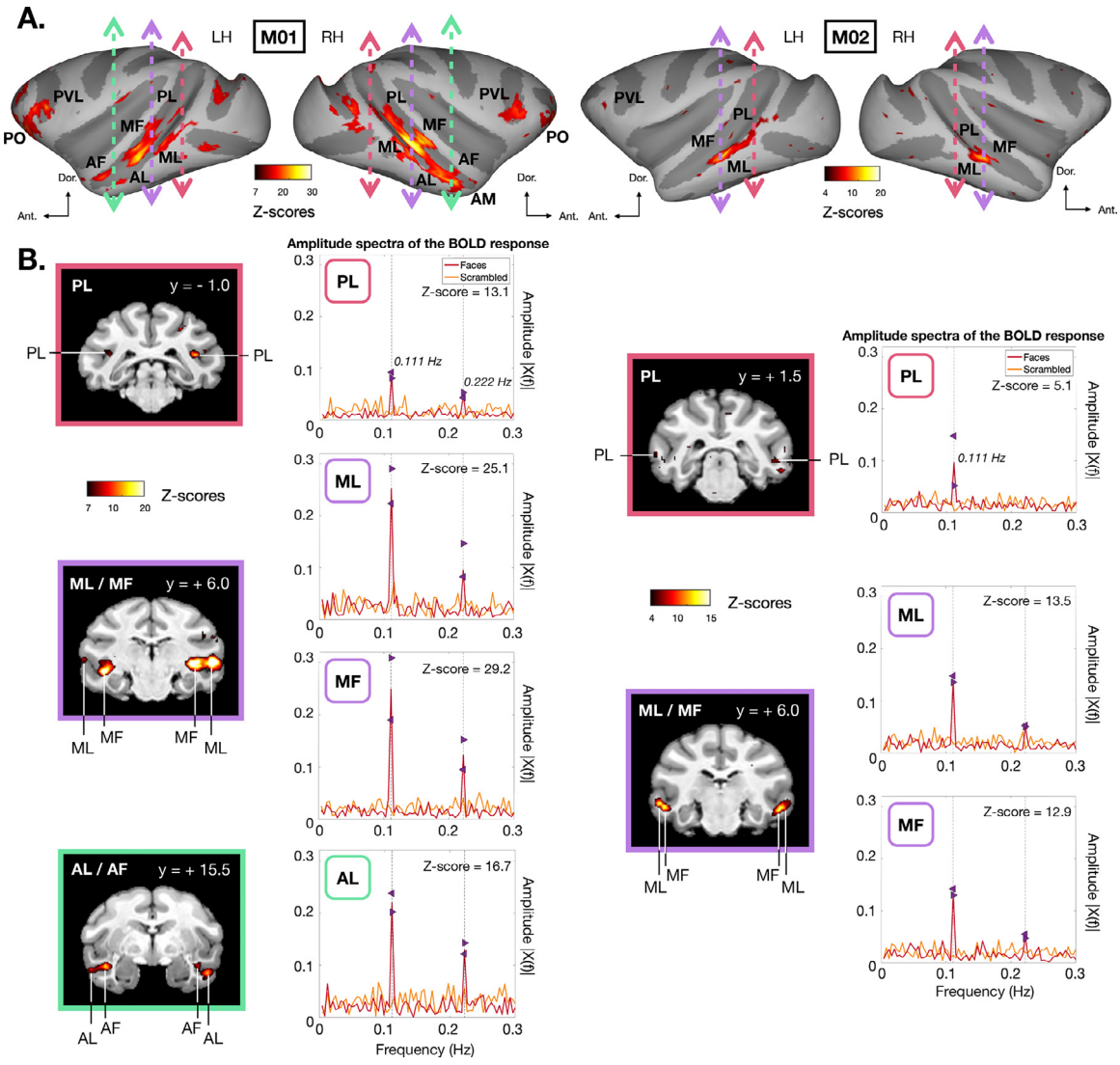

Fig. 3. Face-selective clusters in the STS of macaque monkeys. (A) Significant face-selective activations projected on the inflated cortical hemispheres of M01 (leftward column) and M02 (rightward column). Data were thresholded at $Z = 7$ for M01 and $Z = 4$ for M02. Ant.: anterior, Dor.: dorsal, LH: left hemisphere, RH: right hemisphere. **(B)** STS face-selective clusters. Z-scores are shown on coronal slices selected on the volumetric space (leftwards columns). The dotted lines in panel A give the positions of these slices on the cortical surfaces of each monkey. Their Y-coordinates in the MNI space are provided in the upper-right corner of each slice. The amplitude spectra of the BOLD responses around the local maxima of each face-selective cluster are shown on the rightward panels for face stimuli (in red) and their phase-scrambled controls (in orange). Note the high SNR of the activity at 0.111 Hz and 0.222 Hz. These data were averaged across the two hemispheres for each monkey. The vertical gray dotted lines indicate the first ($F = 0.11$ Hz) and second ($2F = 0.222$ Hz) harmonics of the face stimulation frequency. The left and right arrows provide amplitude values in the left and right hemispheres at these harmonics. The averaged SNRs at the local maxima in both hemispheres are provided in the upper-right corner of each graph.

clusters between the two monkeys. This variability is not related to the values used to threshold the Z-scores maps (see Supplementary Fig. 3) and actually reflects a genuine difference between the cortical face networks of the two macaques. This finding agrees with the inter-subject variability observed in previous macaque studies (Tsao et al., 2008a; Ku et al., 2011) as well as in humans (e.g., Rossion et al., 2012; Zhen et al., 2015; with the present localizer: Gao et al., 2022).

Importantly, our approach also achieves high test-retest reliability in localizing face-selective areas in both animals since the calculated Dice indexes (see Section 2.4.5.) are all moderate to high (0.60–0.79; as described in Wilson et al., 2016) (the Z-scores maps used to compute these indexes are shown in Supplementary Fig. 4). At a threshold level of $Z = 3$, the face-selective nodes identified in the anatomically defined STS of odd and even runs reach a Dice index of 0.74 for M01 and 0.68 for M02, and these coefficients were still very high at the thresholds depicted in Figs. 3 and 4 where the values reach 0.72 for M01 and 0.73 for M02. At the whole-brain level, consistency values also reach 0.66 for M01 and 0.62 for M02 at a threshold of $Z = 3$, 0.77 for M01, and 0.61 for M02 when increasing the thresholds to those in Figs. 3 and 4. It is important to note that these consistency values are higher than the typical range reported in previous human fMRI studies (Duncan et al., 2009; Duncan and Devlin, 2011) and, to the best of our knowledge, constitute the first high test-retest reliability values reported in monkey fMRI studies (see Table 2).

Our data were very reproducible at the individual level, as also assessed by a correlation analysis performed between the Z-scores obtained in the STS of the odd and even runs of our two animals, for the activation maps thresholded at $Z = 3$ ($R = 0.82$, P-value $< 10^{-15}$ in M01 and $R = 0.80$, P-value $< 10^{-15}$ in M02), and at the same thresholds as shown in Figs. 3 and 4 for each animal ($R = 0.81$, P-value $< 10^{-15}$ in M01 and $R = 0.81$; P-value $< 10^{-15}$ in M02). Correlation analyses confirmed again that the activations for our two animals were very similar

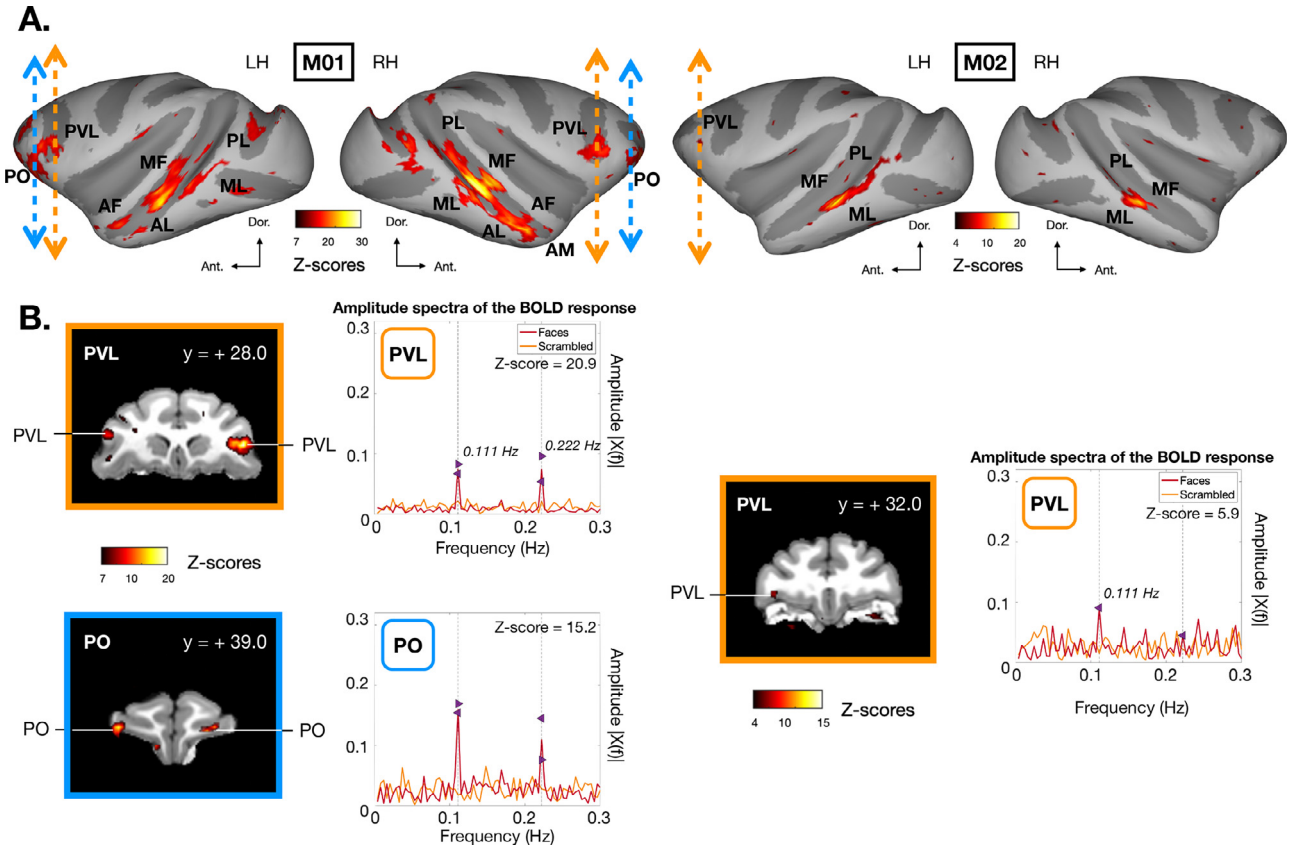

Fig. 4. Face-selective clusters in the prefrontal cortex of macaque monkeys. (A) Z-scores projected on the inflated cortical hemispheres of M01 (leftward column) and M02 (rightward column). PVL: Prefrontal Ventrolateral, PO: Prefrontal Orbital. Ant.: anterior, Dor.: dorsal, LH: left hemisphere, RH: right hemisphere. **(B)** Specificity of the activations in face-selective clusters of the prefrontal cortex. See Fig. 3 for more details.

Table 2
Test-retest reliability of face-selective nodes in activation maps. The Dice indices and the correlation scores (R) were obtained in the STS defined for each animal and at the whole-brain level, at a threshold of $Z = 3$, and for the thresholds described in Figs. 3 and 4 ($Z = 7$ for M01 and $Z = 4$ for M02). Correlation scores were all associated with a P-value $< 10^{-15}$.

			M01	M02
STS	$Z = 3$	Dice	0.74	0.68
		R	0.82	0.80
	Figure thresholded ($Z = 7$ for M01 and $Z = 4$ for M02)	Dice	0.72	0.73
		R	0.81	0.81
Whole-brain level	$Z = 3$	Dice	0.66	0.62
		R	0.60	0.64
	Figure thresholded ($Z = 7$ for M01 and $Z = 4$ for M02)	Dice	0.77	0.61
		R	0.70	0.53

between odd and even runs at the whole-brain level: for the activations thresholded at $Z = 3$ ($R = 0.60$, P-value $< 10^{-15}$ in M01 and $R = 0.64$, P-value $< 10^{-15}$ in M02) and at the thresholds in Figs. 3 and 4 ($R = 0.70$, P-value $< 10^{-15}$ in M01 and $R = 0.53$, P-value $< 10^{-15}$ in M02).

3.2. Activations in face-selective clusters

Next, we examine whether responses in face-selective clusters can be partly elicited by lower-level visual attributes. Figs. 3-B and 4-B present the amplitude spectra estimated from a Fourier transform of the BOLD responses around the local maxima of each cluster for our main stimuli (in red) and their phase-scrambled controls (in orange). These data were averaged across the left and right hemispheres. For the face stimuli, clear peaks can be observed at the first ($F = 0.111$ Hz) and second ($2F = 0.222$ Hz) harmonics of the face stimulation frequency. Amplitude values for the left and right hemispheres at these frequencies are provided by the left and right arrows, respectively (the associated amplitude spectra are provided in Supplementary Fig. 5).

Consequently, very high SNRs are obtained in these clusters (see the values in the upper-right corners). On the other hand, we did not observe any significant peak at the harmonics of the stimulation frequency for the phase-scrambled control conditions (the associated maps for the phase-scrambled condition are shown in Supplementary Fig. 6), which implies that low-level visual cues do not drive the responses obtained in the main condition. These results were verified statistically in face-selective clusters of the STS and the prefrontal cortex (Fig. 5). Note that in this case, we used face-selective clusters defined from the odd runs (see Supplementary Fig. 4) and performed statistics with Z-scores estimated on the even runs to avoid double-dipping (see Section 2.2.4.). The responses obtained for faces were significantly higher than responses obtained in the phase-scrambled condition (i.e., Z-score differences were greater than 3) in all clusters characterized for both animals.

In terms of sensitivity, our approach led to significant responses even when considering a few runs per animal. Fig. 6 shows the evolution of Z-scores within each face-selective cluster of the STS as a function of the number of runs acquired for each monkey. We obtained Z-scores higher than 3 (equivalent to a P-value < 0.001) from only 5 runs in the ML and MF clusters for M01 and M02 but also in the AL cluster for M01. To localize all face-selective clusters in the STS, only 12 runs were required for M01 and 18 runs for M02.

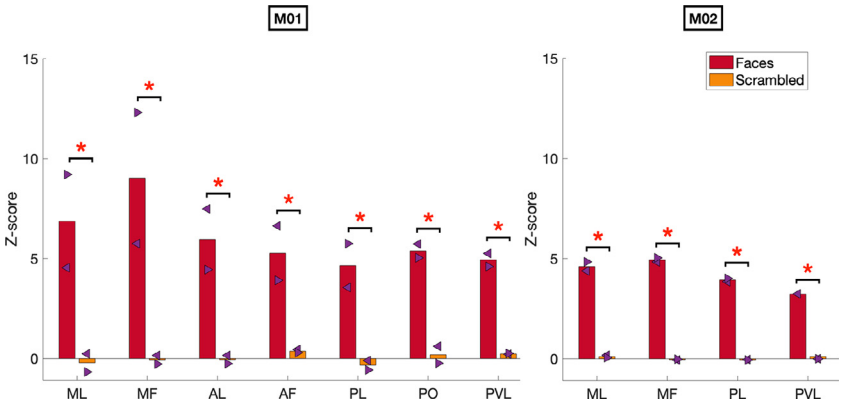

Fig. 5. Comparison between the responses for the face stimuli and their phase-scrambled controls. Z-scores within each face-selective cluster in response to faces (in red) or phase-scrambled images (in orange). These data were averaged across the two hemispheres for each monkey and the left and right arrows provide values for the left and right hemispheres. Red stars indicate a significant difference (i.e., a Z-score difference greater than 3) between activations for faces and their phase-scrambled controls.

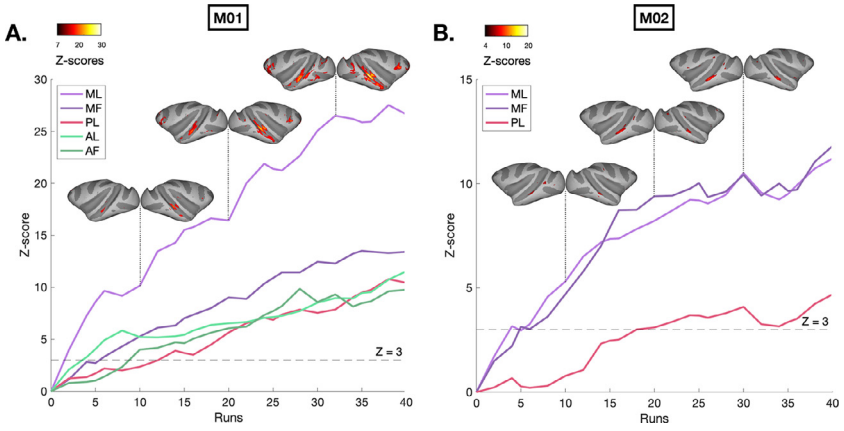

Fig. 6. Evolution of Z-scores in face-selective clusters of the STS as a function of the number of runs. For each cluster in monkey M01 **(A)** and M02 **(B)**, Z-scores were averaged across the two hemispheres. The cortical maps corresponding to 10, 20 and 30 runs are shown on the top. These maps were thresholded using the same values as in Figs. 3 and 4 to facilitate comparison.

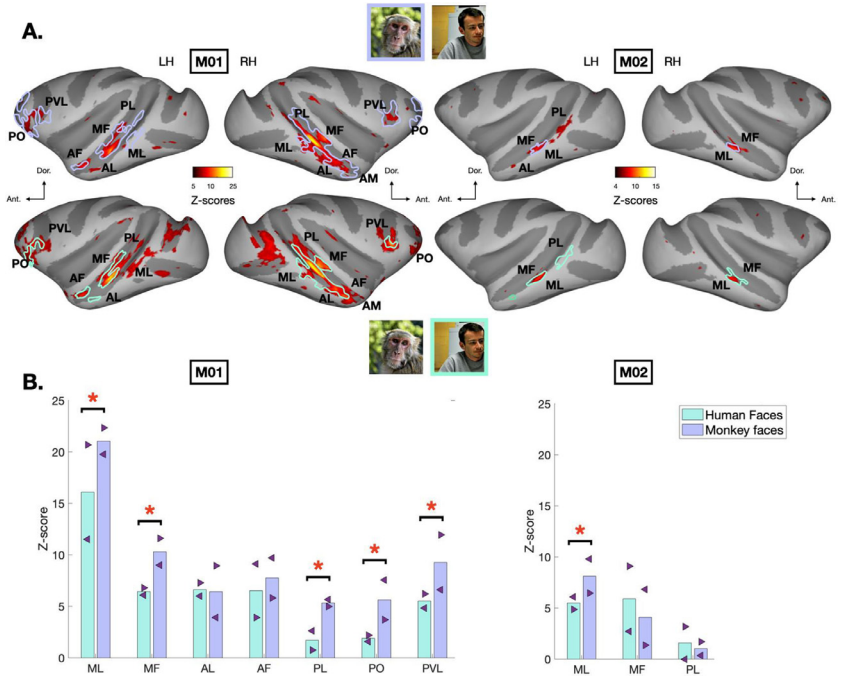

Fig. 7. Comparison between the cortical face networks obtained in response to human and monkey faces. (A) Z-scores associated with human (upper row) and monkey (lower row) faces are projected on the inflated cortical hemispheres of M01 (leftward column) and M02 (rightward column). To facilitate the comparison between the two cortical face networks, the contours of the clusters obtained with human and monkey faces are respectively shown in cyan (lower row) and purple (upper row). See Fig. 3 for more details. **(B)** Z-scores within each face-selective cluster in response to human (cyan) or monkey (purple) faces. The left and right arrows provide values in the left and right hemispheres. Red stars indicate a significant difference (i.e., a Z-score difference greater than 3) between activations for human and monkey faces.

3.3. Responses to human and monkey faces

Finally, we investigate the responses of the face-selective clusters to human and monkey faces, tested across interleaved runs. Fig. 7-A presents the corresponding activations on inflated reconstructions of the left and right cortical hemispheres of M01 and M02. Z-scores in response to human and monkey faces are respectively shown on the upper and lower rows (colored contours of these activation maps are provided to facilitate the comparison). We can observe that the two networks overlap well and are generally associated with similar activations. Although the maps shown here were computed from half the data, they are in excellent agreement with those reported during the analysis of the entire

dataset (see Section 3.1.) with face-selective clusters along the STS on both animals and in the prefrontal cortex in M01 and M02 to a lesser degree.

Even though the extents of the networks obtained for the two conditions appear to be similar, their activations could be more robust for one condition or the other in some face-selective areas. Fig. 7-B provides the Z-scores elicited by human (cyan) and monkey (purple) faces around the local maximum of each face-selective cluster. For each condition, these local maxima were defined from the data collected with the other condition to avoid double-dipping effects (see the "Material and Methods" section). The MNI coordinates of these local maxima are provided in Supplementary Table 1. Activations to human and monkey faces were rather similar within the face-selective clusters identified in both monkeys. However, we found that responses to monkey faces were significantly higher than responses to human faces in the ML cluster for both M01 and M02. In M01, stronger responses to monkey faces were also observed in the PL and MF clusters of the STS and the prefrontal cortex (clusters PVL and PO).

4. Discussion

4.1. The value of comparable cross-species fMRI localizers

Functional localizers in fMRI have become standard for understanding the neural mechanisms underlying cognitive functions, notably face recognition (Saxe et al., 2006; Kanwisher, 2017). They permit identifying regions of interest (ROIs) associated with a given experimental contrast to subsequently compare the responses within these ROIs between human participants (without normalizing the data to a common template) and experimental conditions. Many functional localizers of the cortical face network have been used in humans (e.g., Kanwisher et al., 1997; Ishai et al., 2005; Fox et al., 2009; Berman et al., 2010; Rossion et al., 2012; Weiner and Grill-Spector, 2013; Zhen et al., 2015; Kanwisher, 2017; Gao et al., 2018). This approach has also been adopted in macaques to compare this species' cortical face network to humans (Tsao et al., 2008a,b; Pinsk et al., 2009; Mantini et al., 2012; Yovel and Freiwald, 2013; Weiner and Grill-Spector, 2015; see also Hung et al., 2015; Schaeffer et al., 2020 in marmosets) and to characterize face-selective cellular level activity with invasive neurophysiological recordings or microstimulations (Tsao et al., 2006; Moeller et al., 2008; Freiwald et al., 2009; Freiwald and Tsao, 2010; Issa and DiCarlo, 2012; Taubert et al., 2015; Aparicio et al., 2016; Chang and Tsao, 2017; Moeller et al., 2017; Taubert et al., 2018). However, many parameters of these fMRI localizers differ between studies and species, limiting the reproducibility of the results and the validity of the comparison between humans and macaques. As a key example, Tsao et al. (2008)'s comparison of the cortical face network in the two species is limited by substantial methodological differences between the MRI sequences performed (multi-echo for monkeys versus standard EPI for humans), the acquisition duration (longer TR for monkeys than for humans), MRI slice orientation (coronal for monkeys vs. axial for humans) and, as typically performed in macaque fMRI studies, an injected contrast agent (MION) (vs. the BOLD response in humans). Beyond genuine anatomo-functional differences between the brains of these two species, in particular in the temporal lobe (Rilling and Seligman, 2002; Bryant and Preuss, 2018), these methodological differences may be partly responsible for differences observed in terms of localization of activation and response properties of their respective cortical face networks (Yovel and Freiwald, 2013; Rossion and Taubert, 2019). In this context of inter-species comparison, it is crucial to provide fMRI localizers for non-human primates that are as similar as possible to those used in humans.

The face localizer evaluated here in macaques to fulfill this aim of optimizing inter-species comparisons was directly adapted from a recently validated human fMRI frequency-tagging paradigm with high sensitivity (i.e., high SNR), specificity and test-retest reliability (Gao et al., 2018, 2019, 2022). Here, as in humans, fMRI recordings were based on gradient-echo EPI sequences, axial acquisitions, and a TR of 1.5 s. No contrast agent was used, therefore recording BOLD responses in monkeys, yet with a very high SNR (see discussion below). Importantly, the frequency-tagging paradigm with periodic "mini-bursts" of faces inserted among a rapid train of non-face objects allowed to objectively identify face-selective activity in the Fourier domain exactly at the stimulation frequency ($F = 0.111$ Hz) and its second harmonic ($2F = 0.222$ Hz), without hemodynamic response function (HRF) modeling. This point is important since the processing of data collected from standard block or event-related designs in fMRI is generally based on an average model of this HRF, ignoring substantial variability of the hemodynamic response between brain regions and individuals (Handwerker et al., 2004; see Cottereau et al., 2017 for data in macaques). Most importantly for the purpose of cross-species comparison, there are genuine differences in HRF between primate species. As a matter of fact, while all or the bulk of the response in most face-selective regions was accounted for by the first harmonic in the human brain (Gao et al., 2018; 2019; 2022), here in macaques the second harmonic is prominent in many regions, especially in the anterior temporal and prefrontal cortices (Figs. 3 and 4). These observations reflect different HRFs among species, brain regions, and individuals that cannot be fully taken into account by differential HRF modeling.

Furthermore, in order to optimize inter-species comparisons, we used identical stimulation parameters for macaques as in humans, i.e., the same stimuli presented at the same rate, with mini-"bursts" of faces inserted every 9 s in the rapid (6 Hz) train of non-face objects. This rapid rate of stimulation ensures only one gaze fixation per image, constrained by the fixation cross, preventing differences in fixation duration between faces and objects (e.g., in monkeys; Guo et al., 2006), own- and other-species of faces (Dahl et al., 2009; Minxha et al., 2017) and between species (Minxha et al., 2017; Wilming et al., 2017). While we cannot exclude that the stimulation frequencies may be better suited for one species than the other and may even be separately optimized for each species in future studies, EEG experiments in humans with this face localizer paradigm show that a relatively broad range of base stimulation frequencies provide the same type of face-selective responses, with 6 Hz being an intermediate (i.e., not too slow, not too fast) frequency value providing high face-selective neural amplitudes (Retter et al., 2020). Moreover, as long as face-selective responses do not overlap in time, the number and relative repetition of non-face object images presented between face exemplars (here between the "bursts" of faces every 9 s) does not affect the amplitude and spatial distribution of the human face-selective response (Retter and Rossion, 2016).

4.2. Typicality of the monkey cortical face network

Importantly, we found significant face-selective neural responses in regions usually identified in previous macaque fMRI studies (Figs. 3 and 4). These responses were primarily localized in the fundus and on the lower bank of the STS in both animals (Fig. 3-A), with the highest activations within the so-called ML and MF clusters, in close agreement with previous monkey fMRI studies (Pinsk et al., 2009; Freiwald and Tsao, 2010). Additional clusters were also observed in the posterior (PL) and anterior (AL, AF, and AM) portions of the STS. These clusters were sometimes confluent, as also reported by other studies (e.g., Tsao et al., 2008a; Janssens et al., 2014 and acknowledged in the review of Hesse and Tsao, 2020), making their delineation challenging. Two additional clusters were localized in the prefrontal lobe (Fig. 4-B) and appear to correspond well to the PVL and PO regions previously reported by Tsao et al. (2008b) and Janssens et al. (2014).

Despite the very high SNR attained in our study, we did not observe any significant face-selective activations in the medial and ventral temporal cortex of our two monkeys (see Supplementary Fig. 2). To our knowledge, only one study identified face-selective activations in these regions, in addition to those already known in the STS, claiming that the ventral clusters may be potential homologs of the human

fusiform face area (FFA; Ku et al., 2011). While the authors of this latter study attributed their original and yet unreplicated findings to increased sensitivity due to high-field (7T) spin-echo imaging, stimulus control was limited in that study, with few categories used and high variability between faces (in terms of gaze directions and facial expressions) not matched for non-face stimuli (either fruits, houses, or fractals). This aspect is often not controlled in other face localizer fMRI studies in which highly homogeneous exemplars are used within a given category, generating substantial category-selective low-level differences (e.g., in stimulus orientation) even when scrambled versions of the stimuli are used (e.g., Tsao et al., 2008a; in humans, see Rossion et al., 2012; Rice et al., 2014; Coggan et al., 2016; Weibert et al., 2018). Here the cortical face networks in our two monkeys were identified from the presentation of a large set of natural (i.e., unsegmented, ecologically valid) images of both faces and objects with high variability in size, orientation, luminance/contrast (of the object/face inside the image), lighting conditions, etc. (Fig. 1; see Supplementary Fig. 1 for a characterization of the low-level properties in these image sets). This variability naturally reduces the potential contributions of low-level visual differences to face-selective neural responses. The lack of any significant activations in all face-selective clusters for the phase-scrambling condition (Figs. 3-B and 4-B) demonstrates that these responses are highly specific, reflecting high-level recognition functions (Rossion et al., 2015; Gao et al., 2018; Or et al., 2019).

Despite this tight (natural) control and the lack of a contrast agent providing a prolonged response function (Pelekanos et al., 2020), our frequency-tagging approach leads to face-selective responses with very high sensitivity (i.e., Z-scores greater than 4 in both monkeys and, up to 29 and 13.5 in the most responsive clusters of M01 and M02 respectively) even when considering a few runs per animal (Fig. 6). For example, while Tsao et al. (2008a) used up to 99 runs in their study, here 20 runs were sufficient to fully characterize the cortical face network of our two macaques. The factors behind the particularly high sensitivity of our fMRI frequency-tagging paradigm have been previously evaluated (i.e., by comparing it directly to a standard face localizer with the same stimuli and total stimulus duration; see Gao et al., 2018) and discussed in details in the original human study: detection of face-selective periodic activity independently of a hemodynamic model fit, noise measurement only in small frequency bins surrounding the signal, limited noise contamination in the frequency bin of interest, maximized contrast without category-adaptation within the mini-"bursts" (see Gao et al., 2018). The contribution of our analysis in the Fourier domain was also investigated by reanalyzing our data using a more classical general linear model (GLM), as in Gao et al. (2018). In this case, face-selective clusters were also identified at similar locations in both animals but SNRs were significantly lower (see the comparison in Supplementary Fig. 7).

4.3. Inter-individual variability and test-retest reliability

There were differences between the spatial extents, anatomical locations, and even the number of face-selective clusters observed in our two macaques. However, we showed that these differences were not caused by the values used to threshold the activation maps (see Supplementary Fig. 3). Since the obtained Z-scores were highly reliable for each animal, this variability appears to reflect a genuine difference between the cortical face networks of the two monkeys. This finding echoes the inter-subject variability observed across monkeys (Pinsk et al., 2009; Janssens et al., 2014; Grimaldi et al., 2016; Arcaro et al., 2020) and human fMRI studies (e.g., Rossion et al., 2012; Gao et al., 2022).

Importantly, our paradigm ensures reliable and reproducible results, as demonstrated by the very good correspondence between the activations obtained from subsets of the data (correlation greater than 0.80 in the STS and Dice index from 0.62 to 0.77 within the whole brain (coefficients all moderate to high) for both monkeys; see Table 2). These reliability tests were inspired by previous human fMRI studies which controlled for robustness, and the values obtained with our paradigm are among the highest reported so far. Correlation scores and Dice indexes should be estimated in future monkey fMRI studies to permit a direct comparison with the reliability obtained with our protocol.

4.4. Human and monkey faces

Another noticeable, although generally neglected, difference between human and monkey face localizers is the stimulus' species. While faces of conspecifics are used in all human fMRI studies, monkeys are tested with either human or monkey faces, without systematic comparison and an unwarranted assumption that this factor has little influence on category-selective brain activations (Russ et al., 2021). Here, one originality of our study is that we used localizers based on either human or monkey faces. Overall, the cortical face networks obtained with these two conditions were very similar (Fig. 7-A), indicating that using human faces in monkeys (raised in captivity) as face localizers is valid to identify face-selective regions (although other face recognition functions, such as eye gaze, emotional expression or identity recognition, may require the use of conspecifics faces; e.g., Taubert et al., 2020). Our results nonetheless indicate that face-selective responses in the ML cluster are more pronounced for monkey faces (advantages for monkey faces were also observed in other clusters of the STS and prefrontal cortex but only in M01). This result will have to be confirmed from data collected in a larger number of macaques, but it is in line with behavioral observations of increased attention and sensitivity to monkey faces compared to human faces in monkeys (Pascalis and Bachevalier, 1998; Dahl et al., 2009; Minxha et al., 2017).

5. Conclusions

Altogether, the present results demonstrate that our functional frequency-tagging face localizer is valid and efficient for characterizing the cortical face network in NHP neuroimaging. The face-selective clusters were objectively identified in both monkeys, in agreement with previous studies. This study opens new possibilities to provide direct comparisons between humans and monkeys using neural signals obtained in an ecologically valid, sensitive, reliable manner, and with identical paradigms. This functional localizer could be applied to further explore different functions in these regions, such as face identity recognition or head orientation and gaze direction processing in primate species (Taubert et al., 2020). Moreover, our frequency-tagging protocol could serve as a template to explore other brain functions. It could also be used in marmoset, which is a rising NHP model in cognitive neurosciences and which can now be used for awake behaving fMRI recordings (Hung et al., 2015; Cléry et al., 2020; Schaeffer et al., 2020). The experimental paradigm, stimuli, and analysis scripts can be found here: https://osf.io/6r8wz/?view_only=3d264c959e4b4d30a114ce2b76f3f079.

Fundings

This research was supported by a grant from the "Agence Nationale de la Recherche" (ANR-16-CE37–0002–01, ANR JCJC 3D3M) awarded to Benoit R. Cottereau, (ANR-18-CE37–0022, ANR CIM2) awarded to Jean-Baptiste Durand and a PhD fellowship from the Université de Lorraine to Marie-Alphée Laurent.

Data availability

Data and analysis codes are accessible at the following link: https://osf.io/6r8wz/?view_only=3d264c959e4b4d30a114ce2b76f3f079.

Credit authorship contribution statement

Marie-Alphée Laurent: Conceptualization, Methodology, Software, Formal analysis, Investigation, Visualization, Writing – original draft,

Writing – review & editing. **Pauline Audurier:** Conceptualization, Methodology, Formal analysis, Investigation, Visualization, Writing – original draft. **Vanessa De Castro:** Investigation, Resources. **Xiaoqing Gao:** Conceptualization, Methodology, Software. **Jean-Baptiste Durand:** Formal analysis, Resources, Writing – review & editing, Funding acquisition. **Jacques Jonas:** Conceptualization, Methodology, Writing – review & editing. **Bruno Rossion:** Conceptualization, Methodology, Writing – original draft, Writing – review & editing, Supervision, Funding acquisition. **Benoit R. Cottereau:** Conceptualization, Methodology, Software, Formal analysis, Investigation, Resources, Writing – original draft, Writing – review & editing, Supervision, Project administration, Funding acquisition.

Acknowledgments

We thank the Inserm/UPS UMR1214 Technical Platform for the MRI acquisitions. We also thank the Animalliance staff for their help with monkey welfare.

Supplementary materials

Supplementary material associated with this article can be found, in the online version, at doi:10.1016/j.neuroimage.2023.119959.

References

Aparicio, P.L., Issa, E.B., DiCarlo, J.J., 2016. Neurophysiological organization of the middle face patch in macaque inferior temporal cortex. J. Neurosci. 36 (50), 12729–12745. doi:10.1523/JNEUROSCI.0237-16.2016.

Arcaro, M.J., Mautz, T., Berezovskii, V.K., Livingstone, M.S., 2020. Anatomical correlates of face patches in macaque inferotemporal cortex. Proc. Natl. Acad. Sci. 117 (51), 32667–32678. doi:10.1073/pnas.2018780117.

Arcaro, M.J., Schade, P.F., Vincent, J.L., Ponce, C.R., Livingstone, M.S., 2017. Seeing faces is necessary for face-domain formation. Nat. Neurosci. 20 (10), 1404–1412. doi:10.1038/nn.4635.

Audurier, P., Héjja-Brichard, Y., De Castro, V., Kohler, P.J., Norcia, A.M., Durand, J.-.B., Cottereau, B.R., 2022. Symmetry processing in the macaque visual cortex. Cereb. Cortex 32 (10), 2277–2290. doi:10.1093/cercor/bhab358.

Bach, M., Meigen, T., 1999. Do's and don'ts in Fourier analysis of steady-state potentials. Doc. Ophthalmol. 99 (1), 69–82. doi:10.1023/a:1002648202420.

Barraclough, N.E., Perrett, D.I., 2011. From single cells to social perception. Philos. Trans. R. Soc. Lond. B, Biol. Sci. 366 (1571), 1739–1752. doi:10.1098/rstb.2010.0352.

Bell, A.H., Hadj-Bouziane, F., Frihauf, J.B., Tootell, R.B.H., Ungerleider, L.G., 2009. Object representations in the temporal cortex of monkeys and humans as revealed by functional magnetic resonance imaging. J. Neurophysiol. 101 (2), 688–700. doi:10.1152/jn.90657.2008.

Bell, A.H., Malecek, N.J., Morin, E.L., Hadj-Bouziane, F., Tootell, R.B.H., Ungerleider, L.G., 2011. Relationship between functional magnetic resonance imaging-identified regions and neuronal category selectivity. J. Neurosci. 31 (34), 12229–12240. doi:10.1523/JNEUROSCI.5865-10.2011.

Berman, M.G., Park, J., Gonzalez, R., Polk, T.A., Gehrke, A., Knaffla, S., Jonides, J., 2010. Evaluating functional localizers : the case of the FFA. Neuroimage 50 (1), 56–71. doi:10.1016/j.neuroimage.2009.12.024.

Bryant, K.L., Preuss, T.M., 2018. A comparative perspective on the human temporal lobe. In: Bruner, E., Ogihara, N., Tanabe, H.C. (Eds.), Digital Endocasts : From Skulls to Brains. Springer Japan, pp. 239–258. doi:10.1007/978-4-431-56582-6_16.

Chang, L., Tsao, D.Y., 2017. The code for facial identity in the primate brain. Cell 169 (6), 1013–1028. doi:10.1016/j.cell.2017.05.011, e14..

Cléry, J.C., Schaeffer, D.J., Hori, Y., Gilbert, K.M., Hayrynen, L.K., Gati, J.S., Menon, R.S., Everling, S., 2020. Looming and receding visual networks in awake marmosets investigated with fMRI. Neuroimage 215, 116815. doi:10.1016/j.neuroimage.2020.116815.

Coggan, D.D., Liu, W., Baker, D.H., Andrews, T.J., 2016. Category-selective patterns of neural response in the ventral visual pathway in the absence of categorical information. Neuroimage 135, 107–114. doi:10.1016/j.neuroimage.2016.04.060.

Cottereau, B.R., McKee, S.P., Norcia, A.M., 2012. Bridging the gap : global disparity processing in the human visual cortex. J. Neurophysiol. 107 (9), 2421–2429. doi:10.1152/jn.01051.2011.

Cottereau, B., Smith, A., Rima, S., Fize, D., Héjja-Brichard, Y., Renaud, L., Lejards, C., Vayssiere, N., Trotter, Y., Durand, J.B., 2017. Processing of egomotion-consistent optic flow in the rhesus macaque cortex. Cereb. Cortex (N. Y. N.Y. : 1991) 27. doi:10.1093/cercor/bhw412.

Dahl, C.D., Logothetis, N.K., Kayser, C., 2009. Spatial organization of multisensory responses in temporal association cortex. J. Neurosci. Off. J. Soc. Neurosci. 29 (38), 11924–11932. doi:10.1523/JNEUROSCI.3437-09.2009.

Desimone, R., 1991. Face-selective cells in the temporal cortex of monkeys. J. Cogn. Neurosci. 3, 1–8. doi:10.1162/jocn.1991.3.1.1.

Duncan, K.J., Pattamadilok, C., Knierim, I., Devlin, J.T., 2009. Consistency and variability in functional localisers. Neuroimage 46 (4), 1018–1026. doi:10.1016/j.neuroimage.2009.03.014.

Fisher, C., Freiwald, W.A., 2015. Contrasting specializations for facial motion within the macaque face-processing system. Curr. Biol. CB 25 (2), 261–266. doi:10.1016/j.cub.2014.11.038.

Fox, C.J., Iaria, G., Barton, J.J.S., 2009. Defining the face processing network : optimization of the functional localizer in fMRI. Hum. Brain Mapp. 30 (5), 1637–1651. doi:10.1002/hbm.20630.

Freiwald, W.A., Tsao, D.Y., Livingstone, M.S., 2009. A face feature space in the macaque temporal lobe. Nat. Neurosci. 12 (9), 1187–1196. doi:10.1038/nn.2363.

Freiwald, W.A., Tsao, D.Y., 2010. Functional compartmentalization and viewpoint generalization within the macaque face-processing system. Science 330 (6005), 845–851. doi:10.1126/science.1194908.

Gao, X., Gentile, F., Rossion, B., 2018. Fast periodic stimulation (FPS) : a highly effective approach in fMRI brain mapping. Brain Struct. Funct. 223 (5), 2433–2454. doi:10.1007/s00429-018-1630-4.

Gao, X., Vuong, Q.C., Rossion, B., 2019. The cortical face network of the prosopagnosic patient PS with fast periodic stimulation in fMRI. Cortex 119, 528–542. doi:10.1016/j.cortex.2018.11.008.

Gao, X., Wen, M., Sun, M., Rossion, B., 2022. A genuine interindividual variability in number and anatomical localization of face-selective regions in the human brain. Cereb. Cortex (N.Y. N.Y.: 1991) 4834–4856. doi:10.1093/cercor/bhab519.

Grimaldi, P., Saleem, K.S., Tsao, D., 2016. Anatomical connections of the functionally-defined "face patches" in the macaque monkey. Neuron 90 (6), 1325–1342. doi:10.1016/j.neuron.2016.05.009.

Gross, C.G., Rocha-Miranda, C.E., Bender, D.B., 1972. Visual properties of neurons in inferotemporal cortex of the Macaque. J. Neurophysiol. 35 (1), 96–111. doi:10.1152/jn.1972.35.1.96.

Guo, K., Mahmoodi, S., Robertson, R. G., Young, M. P., 2006. Longer fixation duration while viewing face images. Experimental Brain Research 171 (1), 91–98. https://doi.org/10.1007/s00221-005-0248-y.

Hadj-Bouziane, F., Bell, A.H., Knusten, T.A., Ungerleider, L.G., Tootell, R.B.H., 2008. Perception of emotional expressions is independent of face selectivity in monkey inferior temporal cortex. Proc. Natl. Acad. Sci. 105 (14), 5591–5596. doi:10.1073/pnas.0800489105.

Handwerker, D.A., Ollinger, J.M., D'Esposito, M, 2004. Variation of BOLD hemodynamic responses across subjects and brain regions and their effects on statistical analyses. Neuroimage 21 (4), 1639–1651. doi:10.1016/j.neuroimage.2003.11.029.

Haxby, J.V., Ungerleider, L.G., Clark, V.P., Schouten, J.L., Hoffman, E.A., Martin, A., 1999. The effect of face inversion on activity in human neural systems for face and object perception. Neuron 22 (1), 189–199. doi:10.1016/s0896-6273(00)80690-x.

Haxby, J.V., Hoffman, E.A., Gobbini, M.I., 2000. The distributed human neural system for face perception. Trends Cogn. Sci. (Regul. Ed.) doi:10.1016/S1364-6613(00)01482-0.

Héjja-Brichard, Y., Rima, S., Rapha, E., Durand, J.-.B., Cottereau, B.R., 2020. Stereomotion processing in the nonhuman primate brain. Cereb. Cortex 30 (8), 4528–4543. doi:10.1093/cercor/bhaa055.

Hesse, J.K., Tsao, D.Y., 2020. The macaque face patch system : a turtle's underbelly for the brain. Nat. Rev. Neurosci. 21 (12), 695–716. doi:10.1038/s41583-020-00393-w.

Honey, C., Kirchner, H., VanRullen, R., 2008. Faces in the cloud : fourier power spectrum biases ultrarapid face detection. J. Vis. 8 (12), 9.1–913. doi:10.1167/8.12.9.

Hung, C.C., Yen, C.C., Ciuchta, J.L., Papoti, D., Bock, N.A., Leopold, D.A., Silva, A.C., 2015. Functional mapping of face-selective regions in the extrastriate visual cortex of the marmoset. J. Neurosci. Off. J. Soc. Neurosci. 35 (3), 1160–1172. doi:10.1523/JNEUROSCI.2659-14.2015.

Ishai, A., Schmidt, C.F., Boesiger, P., 2005. Face perception is mediated by a distributed cortical network. Brain Res. Bull. 67 (1–2), 87–93. doi:10.1016/j.brainresbull.2005.05.027.

Ishai, A., 2008. Let's face it : it's a cortical network. Neuroimage 40 (2), 415–419. doi:10.1016/j.neuroimage.2007.10.040.

Issa, E.B., DiCarlo, J.J., 2012. Precedence of the eye region in neural processing of faces. J. Neurosci. Off. J. Soc. Neurosci. 32 (47), 16666–16682. doi:10.1523/JNEUROSCI.2391-12.2012.

Jacobsen, C.F., 1936. Studies of cerebral function in primates. I. The functions of the frontal association areas in monkeys. Compar. Psychol. Monogr. 13 (3), 1–60.

Janssens, T., Zhu, Q., Popivanov, I.D., Vanduffel, W., 2014. Probabilistic and single-subject retinotopic maps reveal the topographic organization of face patches in the macaque cortex. J. Neurosci. 34 (31), 10156–10167. doi:10.1523/JNEUROSCI.2914-13.2013.

Jonas, J., Jacques, C., Liu-Shuang, J., Brissart, H., Colnat-Coulbois, S., Maillard, L., Rossion, B., 2016. A face-selective ventral occipito-temporal map of the human brain with intracerebral potentials. Proc. Natl. Acad. Sci. 113. doi:10.1073/pnas.1522033113.

Kanwisher, N., McDermott, J., Chun, M.M., 1997. The fusiform face area : a module in human extrastriate cortex specialized for face perception. J. Neurosci. Off. J. Soc. Neurosci. 17 (11), 4302–4311. doi:10.1523/JNEUROSCI.17-11-04302.1997.

Kanwisher, N., 2017. The quest for the FFA and where it led. J. Neurosci. 37 (5), 1056–1061. doi:10.1523/JNEUROSCI.1706-16.2016.

Kawabata Duncan, K.J., Devlin, J.T., 2011. Improving the reliability of functional localizers. Neuroimage 57 (3), 1022–1030. doi:10.1016/j.neuroimage.2011.05.009.

Kriegeskorte, N., Simmons, W.K., Bellgowan, P.S.F., Baker, C.I., 2009. Circular analysis in systems neuroscience : the dangers of double dipping. Nat. Neurosci. 12 (5). doi:10.1038/nn.2303, Art. 5..

Krug, K., Parker, A.J., 2017. The neural events that change perception. e-Neuroforum 24 (1), A31–A39. doi:10.1515/nf-2017-A036.

Ku, S.P., Tolias, A.S., Logothetis, N.K., Goense, J., 2011. FMRI of the face-processing network in the ventral temporal lobe of awake and anesthetized macaques. Neuron 70 (2), 352–362. doi:10.1016/j.neuron.2011.02.048.

Lafer-Sousa, R., Conway, B.R., 2013. Parallel, multi-stage processing of colors, faces and shapes in macaque inferior temporal cortex. Nat. Neurosci. 16 (12), 1870–1878. doi:10.1038/nn.3555.

Landi, S.M., Freiwald, W.A., 2017. Two areas for familiar face recognition in the primate brain. Science 357 (6351), 591–595. doi:10.1126/science.aan1139.

Leite, F.P., Tsao, D., Vanduffel, W., Fize, D., Sasaki, Y., Wald, L.L., Dale, A.M., Kwong, K.K., Orban, G.A., Rosen, B.R., Tootell, R.B.H., Mandeville, J.B., 2002. Repeated fMRI using iron oxide contrast agent in awake, behaving macaques at 3 tesla. Neuroimage 16 (2), 283–294. doi:10.1006/nimg.2002.1110.

Livingstone, M.S., Vincent, J.L., Arcaro, M.J., Srihasam, K., Schade, P.F., Savage, T., 2017. Development of the macaque face-patch system. Nat. Commun. 8, 14897. doi:10.1038/ncomms14897.

Mantini, D., Hasson, U., Betti, V., Perrucci, M.G., Romani, G.L., Corbetta, M., Orban, G.A., Vanduffel, W., 2012. Interspecies activity correlations reveal functional correspondence between monkey and human brain areas. Nat. Methods 9 (3), 277–282. doi:10.1038/nmeth.1868.

McCarthy, G., Spicer, M., Adrignolo, A., Luby, M., Gore, J., Allison, T., 1994. Brain activation associated with visual motion studied by functional magnetic resonance imaging in humans. Hum. Brain Mapp. 2 (4), 234–243. doi:10.1002/hbm.460020405.

McLaren, D.G., Kosmatka, K.J., Oakes, T.R., Kroenke, C.D., Kohama, S.G., Matochik, J.A., Ingram, D.K., Johnson, S.C., 2009. A population-average MRI-based atlas collection of the rhesus macaque. Neuroimage 45 (1), 52–59. doi:10.1016/j.neuroimage.2008.10.058.

McLaren, D.G., Kosmatka, K.J., Kastman, E.K., Bendlin, B.B., Johnson, S.C., 2010. Rhesus macaque brain morphometry : a methodological comparison of voxel-wise approaches. Methods 50 (3), 157–165. doi:10.1016/j.ymeth.2009.10.003.

Minxha, J., Mosher, C., Morrow, J.K., Mamelak, A.N., Adolphs, R., Gothard, K.M., Rutishauser, U., 2017. Fixations gate species-specific responses to free viewing of faces in the human and macaque amygdala. Cell Rep. 18 (4), 878–891. doi:10.1016/j.celrep.2016.12.083.

Moeller, S., Freiwald, W.A., Tsao, D.Y., 2008. Patches with links : a unified system for processing faces in the macaque temporal lobe. Science 320 (5881), 1355–1359. doi:10.1126/science.1157436.

Moeller, S., Crapse, T., Chang, L., Tsao, D.Y., 2017. The effect of face patch microstimulation on perception of faces and objects. Nat. Neurosci. 20 (5), 743–752. doi:10.1038/nn.4527.

Murphy, A.P., Leopold, D.A., 2019. A parameterized digital 3D model of the Rhesus macaque face for investigating the visual processing of social cues. J. Neurosci. Methods 324, 108309. doi:10.1016/j.jneumeth.2019.06.001.

Or, C.C.F., Retter, T.L., Rossion, B., 2019. The contribution of color information to rapid face categorization in natural scenes. J. Vis. 19 (5), 20. doi:10.1167/19.5.20.

Orban, G.A., Van Essen, D., Vanduffel, W., 2004. Comparative mapping of higher visual areas in monkeys and humans. Trends Cogn. Sci. (Regul. Ed.) 8 (7), 315–324. doi:10.1016/j.tics.2004.05.009.

Pascalis, O., Bachevalier, J., 1998. Face recognition in primates : a cross-species study. Behav. Process. 43 (1), 87–96. doi:10.1016/s0376-6357(97)00090-9.

Passingham, R., 2009. How good is the macaque monkey model of the human brain? Curr. Opin. Neurobiol. 19 (1), 6–11. doi:10.1016/j.conb.2009.01.002.

Pelekanos, V., Mok, R.M., Joly, O., Ainsworth, M., Kyriazis, D., Kelly, M.G., Bell, A.H., Kriegeskorte, N., 2020. Rapid event-related, BOLD fMRI, non-human primates (NHP) : choose two out of three. Sci. Rep. 10 (1), 7485. doi:10.1038/s41598-020-64376-8.

Perrett, D.I., Rolls, E.T., Caan, W., 1982. Visual neurones responsive to faces in the monkey temporal cortex. Exp. Brain Res. 47 (3), 329–342. doi:10.1007/BF00239352.

Pinsk, M.A., DeSimone, K., Moore, T., Gross, C.G., Kastner, S., 2005. Representations of faces and body parts in macaque temporal cortex : a functional MRI study. Proc. Natl. Acad. Sci. 102 (19), 6996–7001. doi:10.1073/pnas.0502605102.

Pinsk, M.A., Arcaro, M., Weiner, K.S., Kalkus, J.F., Inati, S.J., Gross, C.G., Kastner, S., 2009. Neural representations of faces and body parts in macaque and human cortex : a comparative fMRI study. J. Neurophysiol. 101 (5), 2581–2600. doi:10.1152/jn.91198.2008.

Premereur, E., Taubert, J., Janssen, P., Vogels, R., Vanduffel, W., 2016. Effective connectivity reveals largely independent parallel networks of face and body patches. Curr. Biol. CB 26 (24), 3269–3279. doi:10.1016/j.cub.2016.09.059.

Puce, A., Allison, T., Gore, J.C., McCarthy, G., 1995. Face-sensitive regions in human extrastriate cortex studied by functional MRI. J. Neurophysiol. 74 (3), 1192–1199. doi:10.1152/jn.1995.74.3.1192.

Puce, A., Allison, T., Asgari, M., Gore, J.C., McCarthy, G., 1996. Differential sensitivity of human visual cortex to faces, letterstrings, and textures : a functional magnetic resonance imaging study. J. Neurosci. 16 (16), 5205–5215. doi:10.1523/JNEUROSCI.16-16-05205.1996.

Rajimehr, R., Young, J.C., Tootell, R.B.H., 2009. An anterior temporal face patch in human cortex, predicted by macaque maps. Proc. Natl. Acad. Sci. 106 (6), 1995–2000. doi:10.1073/pnas.0807304106.

Regan, D., 1966. Some characteristics of average steady-state and transient responses evoked by modulated light. Electroencephalogr. Clin. Neurophysiol. 20 (3), 238–248. doi:10.1016/0013-4694(66)90088-5.

Retter, T.L., Rossion, B., 2016. Uncovering the neural magnitude and spatio-temporal dynamics of natural image categorization in a fast visual stream. Neuropsychologia 91, 9–28. doi:10.1016/j.neuropsychologia.2016.07.028.

Retter, T.L., Jiang, F., Webster, M.A., Rossion, B., 2020. All-or-none face categorization in the human brain. Neuroimage 213, 116685. doi:10.1016/j.neuroimage.2020.116685.

Retter, T., Rossion, B., Schiltz, C., 2021. Harmonic amplitude summation for frequency-tagging analysis. J. Cogn. Neurosci. 33, 1–22. doi:10.1162/jocn_a_01763.

Rice, G.E., Watson, D.M., Hartley, T., Andrews, T.J., 2014. Low-level image properties of visual objects predict patterns of neural response across category-selective regions of the ventral visual pathway. J. Neurosci. 34 (26), 8837–8844. doi:10.1523/JNEUROSCI.5265-13.2014.

Rilling, J.K., Seligman, R.A., 2002. A quantitative morphometric comparative analysis of the primate temporal lobe. J. Hum. Evol. 42 (5), 505–533. doi:10.1006/jhev.2001.0537.

Rossion, B., Hanseeuw, B., Dricot, L., 2012. Defining face perception areas in the human brain : a large-scale factorial fMRI face localizer analysis. Brain Cogn. 79 (2), 138–157. doi:10.1016/j.bandc.2012.01.001.

Rossion, B., Torfs, K., Jacques, C., Liu-Shuang, J., 2015. Fast periodic presentation of natural images reveals a robust face-selective electrophysiological response in the human brain. J. Vis. 15 (1), 18. doi:10.1167/15.1.18, -18.

Rossion, B., Jacques, C., Jonas, J., 2018. Mapping face categorization in the human ventral occipitotemporal cortex with direct neural intracranial recordings. Ann. N. Y. Acad. Sci. 1426. doi:10.1111/nyas.13596.

Rossion, B., Taubert, J., 2019. What can we learn about human individual face recognition from experimental studies in monkeys? Vision Res. 157, 142–158. doi:10.1016/j.visres.2018.03.012.

Russ, B.E., Leopold, D.A., 2015. Functional MRI mapping of dynamic visual features during natural viewing in the macaque. Neuroimage 109, 84–94. doi:10.1016/j.neuroimage.2015.01.012.

Russ, B.E., Petkov, C.I., Kwok, S.C., Zhu, Q., Belin, P., Vanduffel, W., Hamed, S.B., 2021. Common functional localizers to enhance NHP & cross-species neuroscience imaging research. Neuroimage 237, 118203. doi:10.1016/j.neuroimage.2021.118203.

Saxe, R., Brett, M., Kanwisher, N., 2006. Divide and conquer : a defense of functional localizers. Neuroimage 30 (4), 1088–1096. doi:10.1016/j.neuroimage.2005.12.062, discussion 1097-1099..

Schaeffer, D.J., Selvanayagam, J., Johnston, K.D., Menon, R.S., Freiwald, W.A., Everling, S., 2020. Face selective patches in marmoset frontal cortex. Nat. Commun. 11 (1), 4856. doi:10.1038/s41467-020-18692-2.

Sergent, J., Ohta, S., MacDonald, B., 1992. Functional neuroanatomy of face and object processing. A positron emission tomography study. Brain A J. Neurol. 1, 15–36. doi:10.1093/brain/115.1.15, *115 Pt*.

Taubert, J., Belle, G.V., Vanduffel, W., Rossion, B., Vogels, R., 2015. Neural correlate of the thatcher face illusion in a monkey face-selective patch. J. Neurosci. 35 (27), 9872–9878. doi:10.1523/JNEUROSCI.0446-15.2015.

Taubert, J., Van Belle, G., Vogels, R., Rossion, B., 2018. The impact of stimulus size and orientation on individual face coding in monkey face-selective cortex. Sci. Rep. 8 (1), 10339. doi:10.1038/s41598-018-28144-z.

Taubert, J., Japee, S., Murphy, A.P., Tardiff, C.T., Koele, E.A., Kumar, S., Leopold, D.A., Ungerleider, L.G., 2020. Parallel processing of facial expression and head orientation in the macaque brain. J. Neurosci. 40 (42), 8119–8131. doi:10.1523/JNEUROSCI.0524-20.2020.

Taubert, J., Wardle, S.G., Tardiff, C.T., Koele, E.A., Kumar, S., Messinger, A., Ungerleider, L.G., 2022. The cortical and subcortical correlates of face pareidolia in the macaque brain. Soc. Cogn. Affect. Neurosci. 965–976. doi:10.1093/scan/nsac031.

Tsao, D.Y., Freiwald, W.A., Knutsen, T.A., Mandeville, J.B., Tootell, R.B.H., 2003. Faces and objects in macaque cerebral cortex. Nat. Neurosci. 6 (9), 989–995. doi:10.1038/nn1111.

Tsao, D.Y., Freiwald, W.A., Tootell, R.B.H., Livingstone, M.S., 2006. A cortical region consisting entirely of face-selective cells. Science 311 (5761), 670–674. doi:10.1126/science.1119983.

Tsao, D.Y., Moeller, S., Freiwald, W.A., 2008a. Comparing face patch systems in macaques and humans. Proc. Natl. Acad. Sci. U. S. A. 105 (49), 19514–19519. doi:10.1073/pnas.0809662105.

Tsao, D.Y., Schweers, N., Moeller, S., Freiwald, W.A., 2008b. Patches of face-selective cortex in the macaque frontal lobe. Nat. Neurosci. 11 (8), 877–879. doi:10.1038/nn.2158.

Van Essen, D.C., Drury, H.A., Dickson, J., Harwell, J., Hanlon, D., Anderson, C.H., 2001. An integrated software suite for surface-based analyses of cerebral cortex. J. Am. Med. Inf. Assoc. JAMIA 8 (5), 443–459. doi:10.1136/jamia.2001.0080443.

Vanduffel, W., Farivar, R., 2014. Functional MRI of awake behaving macaques using standard equipment. Advanced Brain Neuroimaging Topics in Health and Disease—Methods and Applications. IntechOpen doi:10.5772/58281.

Weibert, K., Flack, T.R., Young, A.W., Andrews, T.J., 2018. Patterns of neural response in face regions are predicted by low-level image properties. Cortex 103, 199–210. doi:10.1016/j.cortex.2018.03.009.

Weiner, K.S., Grill-Spector, K, 2013. Neural representations of faces and limbs neighbor in human high-level visual cortex : evidence for a new organization principle. Psychol. Res. 77 (1), 74–97. doi:10.1007/s00426-011-0392-x.

Weiner, K.S., Grill-Spector, K, 2015. The evolution of face processing networks. Trends Cogn. Sci. (Regul. Ed.) 19 (5), 240–241. doi:10.1016/j.tics.2015.03.010.

Wilming, N., Kietzmann, T.C., Jutras, M., Xue, C., Treue, S., Buffalo, E.A., König, P., 2017. Differential contribution of low- and high-level image content to eye movements in monkeys and humans. Cereb. Cortex (New York, N.Y.: 1991) 27 (1), 279–293. doi:10.1093/cercor/bhw399.

Wilson, S.M., Bautista, A., Yen, M., Lauderdale, S., Eriksson, D.K., 2016. Validity and reliability of four language mapping paradigms. NeuroImage Clin. 16, 399–408. doi:10.1016/j.nicl.2016.03.015.

Yovel, G., Freiwald, W.A., 2013. Face recognition systems in monkey and human : are they the same thing? F1000Prime Rep. 5, 10. doi:10.12703/P5-10.

Zhen, Z., Yang, Z., Huang, L., Kong, X.Z., Wang, X., Dang, X., Huang, Y., Song, Y., Liu, J., 2015. Quantifying interindividual variability and asymmetry of face-selective regions : a probabilistic functional atlas. Neuroimage 113, 13–25. doi:10.1016/j.neuroimage.2015.03.010.